Strain-hardenability of new strengthened TRIP/TWIP titanium alloys

Y. Danard[a,b], L. Lilensten[a,1], F. Sun[a], P. Vermaut[a], I. Freiherr Von Thüngen[c], G. Martin[d], N. Bozzolo[e], F. Prima[a]

[a] PSL Research University, Chimie ParisTech, Institut de Recherche de Chimie Paris, CNRS UMR 8247, 75005 PARIS, France

[b] TIMET Savoie, 62 Avenue Paul Girod, 73400 Ugine, France

[c] SAFRAN TECH, Rue des Jeunes Bois, Châteaufort - CS 80112 - 78772 Magny-Les-Hameaux, France

[d] Université Grenoble Alpes, CNRS UMR 5266, Grenoble INP, Laboratoire SIMaP, Grenoble, 38000, France

[e] MINES ParisTech, PSL - Research University, CEMEF - Centre de mise en forme des matériaux, CNRS UMR 7635, 06904 Sophia Antipolis Cedex, France

[1] Present address: Max-Planck-Institut für Eisenforschung GmbH, 40237 Düsseldorf, Germany

Abstract

A new Ti-Cr based alloy has been developed to reach a TWIP (TWinning Induced Plasticity) effect as the main deformation mechanism. This new composition, involving Fe addition, was derived from a classical TRIP/TWIP alloy Ti-8.5Cr-1.5Al (wt%) (TCA). The main objective is to achieve an optimized strength/hardenability combination by limiting the TRIP (TRansformation Induced Plasticity) effect whose critical resolved shear stress lowers the plasticity threshold. This new alloy Ti-7Cr-1Al-xFe (wt%) (TCAF) displays excellent mechanical properties, with an increased yield strength (with respect to TCA alloy), a very high work-hardening rate and an extremely high fracture strength (UTS=1415MPa), while maintaining an excellent ductility (ε=0.38 at fracture). Both mechanical (tensile tests) and microstructural characterization at different scales (EBSD, XRD) have been performed, evidencing a dense network of fine {332}<113> mechanical twins as well as the presence of stress-induced martensite plates at twins intersections, as a secondary mechanism.

Introduction

Titanium alloys are increasingly attractive for industrial applications such as aerospace due to their specific properties [1]. However, to fully reach their potential for advanced applications, their ductility (typically below 15%) and their strain-hardening have to be significantly increased. Recently, a new family of β-metastable titanium alloys has been developed, where the combination of TRIP (TRansformation Induced Plasticity), TWIP (TWinning Induced Plasticity) and dislocation glide improve these mechanical properties (ductility around 40% and high work-hardening) [2–12]. Based on the “d-electron alloy design”, initially developed by Morinaga et al. [13–15], the chemical stability of the β phase can be predicted and new “strain transformable” titanium alloys are designed [2]. These new mechanical properties provide a

new area of applications for titanium alloys in aerospace, for instance for components with increased capability to endure damage. Over the last few years, several new TRIP/TWIP titanium alloys have been developed and reported in the literature [2–12]. However, their yield stress generally remains rather low (typically below 600MPa) [2–6,16]. As frequently reported before, the maximum stress required to trigger the martensitic transformation (orthorhombic martensite) is limited [17]. As a consequence, our approach consists in limiting the TRIP effect to improve the yield strength while preserving both strain-hardening rate and uniform ductility. A new alloy, with the following composition Ti-7Cr-1Al-xFe (TCAF)* (wt%), is thus derived from this design strategy, using Fe as a strong β stabilizer to delay the TRIP effect. In addition, Fe is well-known to be an efficient solute strengthening element in Ti-alloys, which can help to further improve the yield strength. The suggested composition is then compared in what follows with a reference alloy whose composition is Ti-8.5Cr-1.5Al (TCA) (wt%) to evaluate only the influence of Fe addition. TCA, reported in our previous studies, is known to be a conventional TRIP/TWIP titanium alloy [18].

Material and experiments

Lab-scale melted TCAF and TCA buttons (200g) were prepared using a tungsten arc-melting furnace under high-purity Ar atmosphere. Ingots were solution-treated at 1173 K for 30 minutes and then water quenched. Specimens were then cold rolled to manufacture sheets, 0.65mm thick, corresponding to a thickness reduction of 80%. Cold-rolled sheets were re-heat treated in the b domain at 1083 K under high purity Ar atmosphere and then water quenched. Thus, the specimens exhibited a fully β recrystallized microstructure with an average grain size of 100µm. Tensile specimens are then extracted from the metal-sheets with gauge dimensions of 50 x 5 x 0.65 mm^3. Uniaxial tensile tests were carried out at room temperature using an INSTRON5966 machine with a 10kN load cell and an external extensometer with a gauge length of 10mm, at a strain rate of 1.7 x 10^{-3} s^{-1}. X-ray diffraction measurements were collected on fractured specimens, using a Bruker Endeavor D8 X-ray diffractometer mounted in the Bragg-Brentano configuration with a Co anode (0.6 mm x 10.5 mm line focus, 35 kV, 28 mA). A TCAF 5% deformed sample was electropolished using a solution of 2-butoxyethanol ($C_6H_{14}O_2$), methanol (CH_3OH), perchloric acid ($HClO_4$) and hydrochloric acid (HCl), held at 278 K. Then, electron backscattered diffraction (EBSD) was performed on the TCAF deformed specimen, using a Bruker Crystalign system mounted onto a Zeiss SUPRA40 field emission gun scanning electron microscope operating at 20kV, with a step size of 94 nm.

Results and discussion

Tensile true stress-true strain curves and the associated work-hardening rates as a function of strain of both TCA and TCAF are presented in Fig. 1. The mechanical properties extracted from Fig. 1 are summarized in Table 1. TCA alloy exhibits typical mechanical properties of TRIP/TWIP titanium alloys commonly found in the literature [2–4] with a combination of high strength (UTS=1100MPa) and high ductility (uniform deformation of 0.42) resulting from a large strain-hardening. TCA stress-strain and work-hardening rate curves show a non-monotonous evolution, involving a typical plateau, due to the activation of different deformation mechanisms, as classically observed in materials with multiple plasticity phenomena [19–21]. The work-hardening rate curve can be split into two domains. In the first stage, from the yield strength to the hump vertex (ε≈0.15), the work-hardening rate increases significantly and in the second stage, from the vertex to

the fracture, it slowly decreases. The shape of the curve is characteristic of TRIP/TWIP titanium alloys, where the first stage corresponds to a combination of strain-induced α'' precipitation, nucleation/growth of twins and dislocation glide. The end of the plateau, corresponding to the vertex on the work-hardening curve, is considered to be the signature of the beginning of plastic deformation of the martensite created during the first stage [22–24]. Lilensten *et al*. followed the deformation of such an alloy with SXRD (Synchrotron X-Ray diffraction) and, showed that the volume fraction of martensite strongly increases during the first stage and then exhibits a slight increase during the second stage. Thus it is assumed that the martensite is mainly formed during the first stage and its volume fraction does not change significantly in the following stage [6].

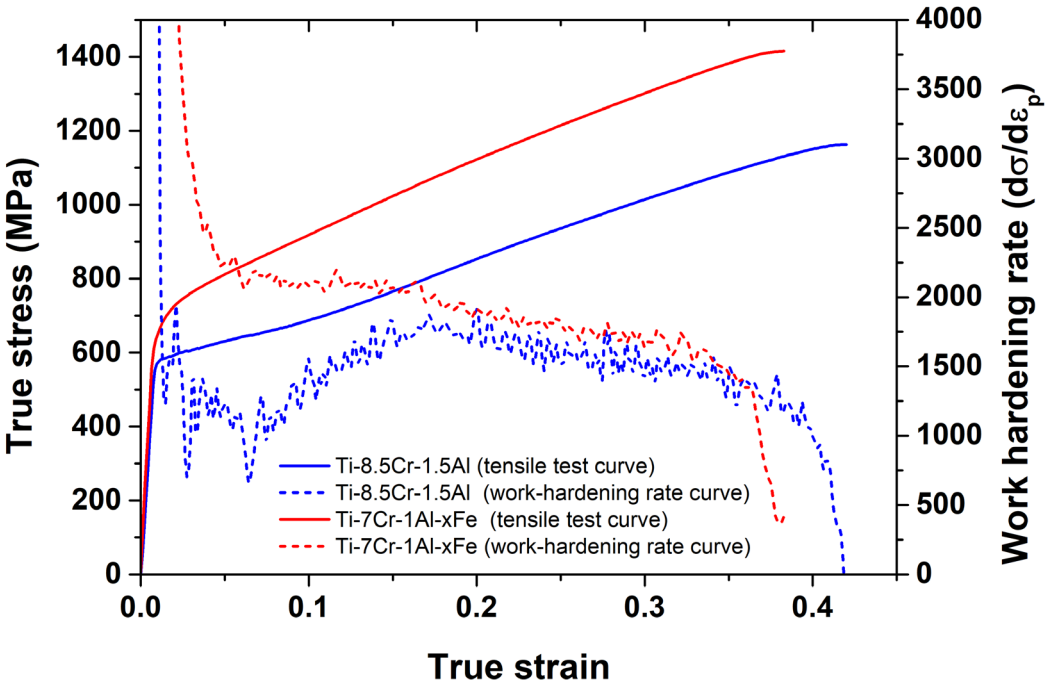

Figure 1 : Tensile true stress-true strain curve of Ti-8.5Cr-1.5Al (wt%) in blue and Ti-7Cr-1Al-xFe (wt%) in red, tested at room temperature at a strain rate of 1.7×10^{-3} s^{-1}. Corresponding work-hardening rate curves as a function of true strain are plotted with dashed lines.

The newly designed alloy, namely TCAF, exhibits excellent mechanical properties with an increase of the yield strength (YS=650MPa) of 80 MPa compared to TCA with same grain size for both alloys, a very high ultimate tensile strength (UTS=1415MPa) and a high work-hardening rate. The improvement of these mechanical properties does not lead to a large loss of ductility (0.38 in uniform deformation). In addition to

the substantial yield strength increase, the main feature of this alloy appears to be its remarkable high strain-hardening. The difference between the ultimate tensile strength and the yield strength (expressed in true stress) for the TCAF is about 765 MPa compared to 590 MPa for the TCA. This value is one of the highest found in the literature in comparison with other β-metastable titanium alloys [2,3,6]. It is worth noting that the TCAF tensile curve shape significantly differs from that of the TCA alloy. Work-hardening rate as a function of strain shows a monotonous decrease, similar to the second stage of usual TRIP/TWIP titanium alloys curves as presented previously. Nevertheless, the work-hardening rate and the stress of TCAF remains larger than, or equal to, the TCA for a given strain value. The difference of shape between TCA and TCAF tensile curves, in particular the absence of plateau for TCAF, where the martensite is supposed to form in large amount, may indicate a difference of deformation mechanisms for TCAF compared to usual TRIP/TWIP titanium alloys such as TCA. These tensile curves suggest that the TRIP effect is no longer the main deformation mechanism in the TCAF, as purposely designed, leading to a yield strength improvement in comparison to TCA without too much impact on the elongation to fracture.

Tableau 1 : Summary of the room temperature tensile properties of Ti-8.5Cr-1.5Al and Ti-7Cr-1Al-xFe tested at a strain rate of 1.7x10-3 s^{-1}

Alloy (wt%)	$\sigma_{0.2}$ (MPa)	UTS (MPa)	ε_{uni}	UTS-YS(MPa)
Ti-8.5Cr-1.5Al (TCA)	570	1160	0.42	590
Ti-7Cr-1Al-xFe (TCAF)	650	1415	0.38	765

XRD diffractograms, shown in Fig.2, are recorded on the surface of fractured tensile specimens for both alloys. Martensite (α'') is clearly detected for TCA but seems to provide much weaker diffracted intensities for TCAF, which confirms the hypothesis made when looking at the shape of the tensile curves, namely that the absence of the plateau indicates that the TRIP effect is not the main deformation mechanism for this alloy. These results also show that martensite transformation is not taking place in large proportions at later stages during the deformation of TCAF. If there is any strain-induced martensite in this alloy, the TRIP effect remains a minor deformation mechanism. It can also be noted that the $(200)_{\beta}$ peak, supposed to be at 66°, is not visible, probably because of the sample texture before and introduced during deformation.

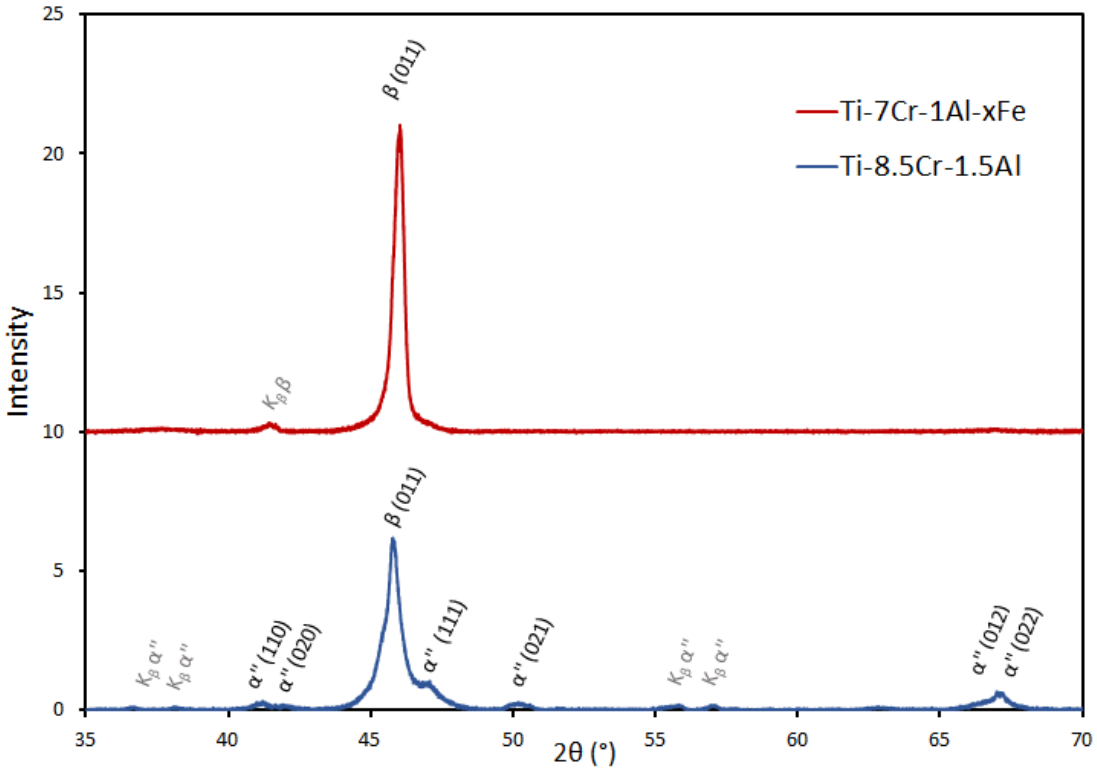

Figure 2 : XRD pattern of Ti-8.5Cr-1.5Al (wt%) in blue and Ti-7Cr-1Al-xFe (wt%) in red, recorded on fractured specimens

EBSD maps of TCAF specimen deformed to a tensile strain of 0.05 are presented in Fig.3. EBSD measurements show that the strain is accommodated by a dense network of twins indexed as {332}<113> in some of the β phase grains. It is admitted in the literature that this profuse twinning reduces the dislocations mean free path, leading to a dynamic Hall-Petch effect, which can account for the high work-hardening of TRIP/TWIP titanium alloys [25].

EBSD phase map seems to exhibit no bands of α'' in the β-matrix similar to the martensite needles of TRIP alloys but shows the presence of α'' within the twins, and especially at the intersection of twin variants. Therefore, in this alloy, α'' martensite, hardly visible on the XRD diffractogram because of its small size and low volume fraction, is not observed as a primary deformation mechanism but is revealed by EBSD as a secondary one. These observations confirm the hypothesis made from the tensile curves, namely, in TCAF, α'' appears only as a secondary deformation mechanism with a very limited volume fraction, typically like in the second stage of usual TRIP/TWIP titanium alloys.

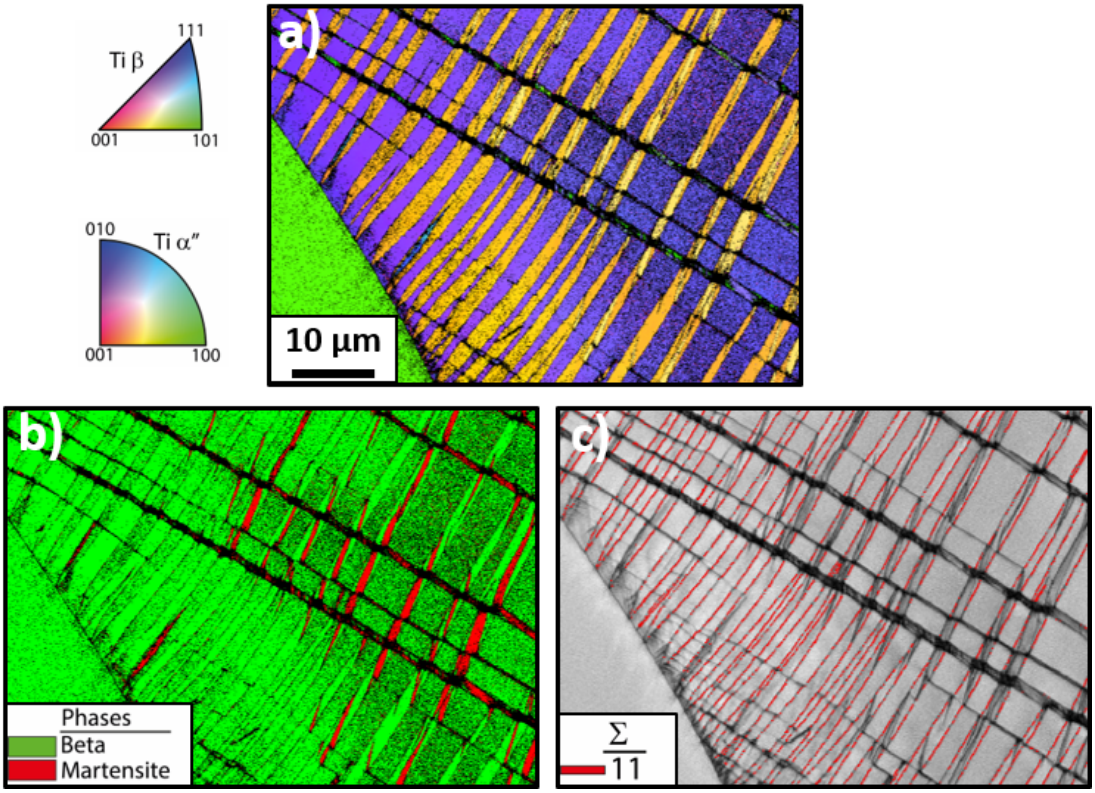

Figure 3 : EBSD analysis of Ti-7Cr-1Al-xFe (wt%) on 5% deformed sample. The tensile axis is horizontal (X axis of the X-Y map). (a) Orientation map with colors indicating the crystallographic direction parallel to the vertical Y axis, as defined onto the standard triangles. (b) Phase map, (c) map of the image quality index of Kikuchi patterns with {332}<113> twin boundaries (CSL Σ11) plotted red

The addition of Fe in the TCAF seems to have stabilized the β phase, leading to an increase of the critical shear stress required to form α'' and thus explains the delay of the TRIP effect. α'' appears as a secondary deformation mechanism and does not limit the yield strength improvement. Lai *et al.* showed that α'' may be the soft phase in these materials, where α'' plates can be cut through by dislocation moving and twin propagation [26]. Regarding the previous conclusion, martensite transformation appears to be an accommodation mechanism taking place at high stress concentration locations, which can contribute to explain the high ductility of TCAF combined with a very high stress level at fracture. These first results open new promising outcomes in the design strategy of TRIP/TWIP titanium alloys, involving fine tuning of mechanical twins as the main strengthening effect and martensitic transformation as an accommodation mechanism.

Conclusion

A new solid-solution strengthened TRIP/TWIP titanium alloy, Ti-7Cr-1Al-xFe, is proposed and the relationship between mechanical properties and deformation mechanisms is highlighted with reference to a conventional TRIP/TWIP alloy Ti-8.5Cr-1.5Al (TCA).

By stabilizing the β phase with Fe addition, it appears that the TRIP effect is triggered only as a secondary deformation mechanism. Combined with its strengthening behavior, the addition of Fe leads to an improvement of the yield strength by 80MPa and a higher work-hardening with a 765MPa difference between the yield strength and the ultimate tensile strength, compared to only 590MPa for TCA (expressed in true stress). The absence of TRIP effect as a primary deformation mechanism is clearly seen on the TCAF work-hardening curve with the suppression of the first stage, compared to the TCA curve. In this alloy, α'', supposed to be the softer phase, is believed to act as an accommodation mechanism and helps to keep a good ductility, while the dense network of thin {332}<113> twins produces a high work-hardening rate thanks to a dynamic Hall-Petch effect.

References

*patent pending

[1] D. Banerjee, J.C. Williams, Acta Materialia 61 (2013) 844–879.

[2] M. Marteleur, F. Sun, T. Gloriant, P. Vermaut, P.J. Jacques, F. Prima, Scripta Materialia 66 (2012) 749–752.

[3] C. Brozek, F. Sun, P. Vermaut, Y. Millet, A. Lenain, D. Embury, P.J. Jacques, F. Prima, Scripta Materialia 114 (2016) 60–64.

[4] F. Sun, J.Y. Zhang, M. Marteleur, C. Brozek, E.F. Rauch, M. Veron, P. Vermaut, P.J. Jacques, F. Prima, Scripta Materialia 94 (2015) 17–20.

[5] F. Sun, J.Y. Zhang, M. Marteleur, T. Gloriant, P. Vermaut, D. Laillé, P. Castany, C. Curfs, P.J. Jacques, F. Prima, Acta Materialia 61 (2013) 6406–6417.

[6] L. Lilensten, Y. Danard, C. Brozek, S. Mantri, P. Castany, T. Gloriant, P. Vermaut, F. Sun, R. Banerjee, F. Prima, Acta Materialia 162 (2019) 268–276.

[7] J. Zhang, J. Li, G. Chen, L. Liu, Z. Chen, Q. Meng, B. Shen, F. Sun, F. Prima, Materials Characterization (n.d.).

[8] L. Ren, W. Xiao, C. Ma, R. Zheng, L. Zhou, Scripta Materialia 156 (2018) 47–50.

[9] S. Sadeghpour, S.M. Abbasi, M. Morakabati, A. Kisko, L.P. Karjalainen, D.A. Porter, Scripta Materialia 145 (2018) 104–108.

[10] M. Ahmed, D. Wexler, G. Casillas, O.M. Ivasishin, E.V. Pereloma, Acta Materialia 84 (2015) 124–135.

[11] X. Min, X. Chen, S. Emura, K. Tsuchiya, Scripta Materialia 69 (2013) 393–396.

[12] P. Castany, T. Gloriant, F. Sun, F. Prima, Comptes Rendus Physique (2018).

[13] M. Abdel-Hady, K. Hinoshita, M. Morinaga, Scripta Materialia 55 (2006) 477–480.

[14] D. Kuroda, M. Niinomi, M. Morinaga, Y. Kato, T. Yashiro, Materials Science and Engineering: A 243 (1998) 244–249.

[15] M. Morinaga, N. Yukawa, T. Maya, K. Sone, H. Adachi, Sixth World Conference on Titanium III 1601 (1988).

[16] Y.-D. Im, Y.-K. Lee, K.-H. Song, Materials Science and Engineering: A (2018).

[17] F. Sun, S. Nowak, T. Gloriant, P. Laheurte, A. Eberhardt, F. Prima, Scripta Materialia 63 (2010) 1053–1056.

[18] Cédrik Brozek, Conception et Développement de Nouveaux Alliages de Titane à Haute Ductilité et Fort Écrouissage, Université Pierre et Marie Curie, 2017.

[19] P.J. Jacques, Q. Furnémont, F. Lani, T. Pardoen, F. Delannay, Acta Materialia 55 (2007) 3681–3693.

[20] F. Lani, Q. Furnémont, T. Van Rompaey, F. Delannay, P.J. Jacques, T. Pardoen, Acta Materialia 55 (2007) 3695–3705.

[21] O. Grässel, L. Krüger, G. Frommeyer, L.W. Meyer, (n.d.).

[22] H.A. Mohamed, J. Washburn, J Mater Sci 12 (1977) 469–480.

[23] J. Perkins, Scripta Metallurgica 8 (1974) 1469–1476.

[24] S. Miyazaki, K. Otsuka, Y. Suzuki, Scripta Metallurgica 15 (1981) 287–292.

[25] B.C. De Cooman, Y. Estrin, S.K. Kim, Acta Materialia 142 (2018) 283–362.

[26] M.J. Lai, T. Li, D. Raabe, Acta Materialia 151 (2018) 67–77.